

## Review Article

# Recent Progress in Hydrogen Electrocatalysis

P. Quaino,<sup>1,2</sup> E. Santos,<sup>1,3</sup> G. Soldano,<sup>1</sup> and W. Schmickler<sup>1</sup>

<sup>1</sup>Institute of Theoretical Chemistry, Ulm University, 89069 Ulm, Germany

<sup>2</sup>PRELINE, Universidad Nacional del Litoral, 3000 Santa Fe, Argentina

<sup>3</sup>Facultad de Matemáticas, Astronomía y Física, IFEG-CONICET, Universidad Nacional de Córdoba, Córdoba, Argentina

Correspondence should be addressed to P. Quaino, paola.quaino@uni-ulm.de

Received 15 February 2011; Accepted 25 March 2011

Academic Editor: Milan M. Jaksic

Copyright © 2011 P. Quaino et al. This is an open access article distributed under the Creative Commons Attribution License, which permits unrestricted use, distribution, and reproduction in any medium, provided the original work is properly cited.

Recently, we have proposed a unified model for electrochemical electron transfer reactions which explicitly accounts for the electronic structure of the electrode. It provides a framework describing the whole course of bond-breaking electron transfer, which explains catalytic effects caused by the presence of surface  $d$  bands. In application on real systems, the parameters of this model—interaction strengths, densities of states, and energies of reorganization—are obtained from density functional theory (DFT). In this opportunity, we review our main achievements in applying the theory of electrocatalysis. Particularly, we have focused on the electrochemical adsorption of a proton from the solution—the Volmer reaction—on a variety of systems of technological interest, such as bare single crystals and nanostructured surfaces. We discuss in detail the interaction of the surface metal  $d$  band with the valence orbital of the reactant and its effect on the catalytic activity as well as other aspects that influence the surface-electrode reactivity such as strain and chemical factors.

## 1. Introduction

The increasing demand for electrical energy and the issues related to environmental pollution have contributed to the development of new technologies for the generation and storage of electrical energy. These technologies focus the attention on the electrochemical devices because of their known advantages (no contamination, usage of renewable resources, low-temperature operation, etc.). In this context, the fuel cell is a promising alternative for the development of new methods of production, conversion, and storage of clean energy. This technology enables direct conversion of chemical energy into electricity; it employs a device in which hydrogen, through reaction with oxygen, produces water and heat as the only products. However, there are still many problems to be solved to ensure that *hydrogen-based systems* become a competitive force.

For decades, a great number of groups worldwide have investigated the hydrogen electrode reaction (HER) experimentally and theoretically in order to improve the electrocatalytic properties of electrode materials and contribute to the general understanding of the hydrogen reaction. For

instance, the role of the electrolyte and the electrode material and the behavior of the reaction intermediate, among others, are the most studied topics.

In this sense, our group has investigated the HER in the framework of a theory for electrocatalysis proposed by two of us (E. Santos and W. Schmickler) [1, 2]. This theory is based on a model Hamiltonian for electrochemical bond breaking reactions [3, 4], which combines ideas of Marcus theory, the Anderson-Newns model [5, 6], and density functional theory (DFT). Hence, realistic calculations for an electrochemical environment can be performed, and the interaction of the valence orbital of the reactant and the  $d$  band of the electrocatalyst, when either fluctuations of the solvent or the applied potential shift their relative positions, can be understood.

On the basis of this Hamiltonian, E. Santos and W. Schmickler have proposed a mechanism [1, 2] by which a metal  $d$  band interacting strongly with the valence level of the reactant may broaden the latter's density of states (DOSs) as it passes the Fermi level and, thereby, enhance the reaction rate. First applications of this idea explained well the trends in the hydrogen electrocatalysis in terms of the position of the metal  $d$  band and its coupling to the hydrogen orbital [7–9].

In this paper, we paper the main contributions we have achieved applying our theory of electrocatalysis. Particularly, we have investigated the hydrogen electrode reaction on several single-crystal surfaces as well as on various nanostructures (clusters, monolayers, nanowires, etc.) on different substrates. We also discuss in detail the role of the position of the metal  $d$  band and its interaction with the  $1s$  hydrogen orbital on the catalytic activity, and finally, we shall explain in detail the contribution of different aspects, such as strain and chemical interactions, on the reactivity of the electrode materials.

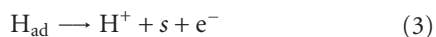
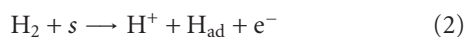
## 2. Mechanism of Electrocatalysis

In order to describe the catalysis mechanism proposed by us (a detailed description of the model can be found in [9]) and the role played by the solvent, we employ an ideal system consisting of the superposition of a wide  $sp$  band with a thin  $d$  band. Two different reactions concerning bond breaking and electron transfer—a reduction and an oxidation reaction—are considered. In both reactions, the bonding orbital of the molecule lies below the Fermi level at the initial state and is filled (Figure 1). In order for the reactions to occur, a thermal fluctuation in the configuration of the solvent must move up (down) the bonding (antibonding) orbital to the Fermi level, so that an electron can be transferred from (to) the reactant to (from) the metal for the oxidation (reduction) process. The resulting ion interacts strongly with the solvent, the solvation shell relaxes towards equilibrium, and, in the final state the bonding (antibonding) orbital lies well above (below) the Fermi level. The most important properties of the metal catalyst that determine their effectivity are the position of the  $d$  band and its coupling strength to the molecular orbitals: a good catalyst usually has a  $d$  band extending across the Fermi level, which interacts strongly with the reactant. When the interaction is weak, the level is just broadened, and when the interaction is strong, the level is split into a bonding and an antibonding orbitals but in this case with respect to the metal. When the overall reaction is in equilibrium, the orbital is half-filled at the transition state and the part of the density of states that lies below the Fermi level reduces the energy of activation. Figure 1 illustrates the described mechanism for the case when  $A \rightarrow A^+ + e^-$ .

In addition, it is important to remark that the same mechanism also operates in other electron transfer reactions.

## 3. Hydrogen Reaction on Single-Crystal Surfaces

It is well known that the hydrogen electrode reaction (HER) consists of the following elementary steps, Tafel (1), Heyrovsky (2), and Volmer (3), respectively:



Therefore the reaction evolves through an adsorbed intermediate ( $\text{H}_{\text{ad}}$ ) on an active site ( $s$ ) on the metal

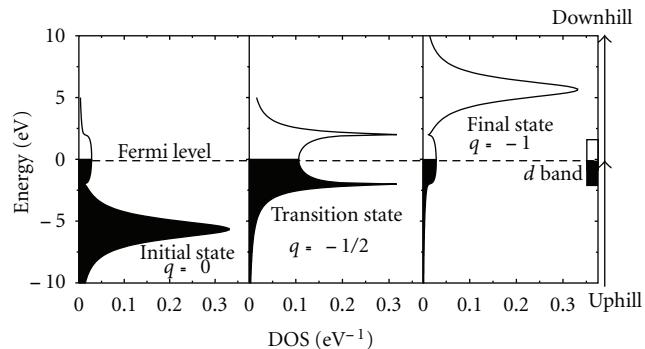


FIGURE 1: Mechanism of electrocatalysis by a  $d$  band near the Fermi level for the following reaction:  $A \rightarrow A^+ + e^-$  on a good metal catalyst: (a) initial, (b) transition, and (c) final states. The Fermi level has been taken as the energy zero.

TABLE 1: Energies of activation for hydrogen adsorption (Volmer step) on various metals [11].

Metal	Cd	Cu	Ag	Au	Pt
$\Delta G_{\text{act}}$ (eV)	0.93	0.71	0.71	0.70	0.30

electrode; and although this is one of the most fundamental reactions in electrochemistry and during the last decades much effort has been spent to clarify the mechanism of electrocatalysis, the behavior of the adsorbed intermediate, the effect of the electrode potential on the adsorbate, the role of the electrolyte, and so forth, there is still a lack of knowledge in understanding the nature of the hydrogen electrocatalysis.

As discussed previously (Sections 1 and 2), a good catalyst has a metal  $d$  band situated at the Fermi level that interacts strongly with the adsorbate and broadens its valence orbital and, thereby, decrease the activation energy. Accordingly, first applications of our theory (for detailed information, see [8, 10, 11]) on the electrochemical adsorption of a proton from the solution onto the surface-Volmer reaction (3)—on good (Pt), mediocre (Au, Ag, Cu), and bad catalysts (Cd) show, as expected, a high activation energy for Cd, medium values for the coin metals, and the lowest one on Pt. The free energy surfaces for the Volmer reaction for four of these metals are shown in Figure 2; the energies of activation are shown in Table 1, and to facilitate the interpretation, the densities of states of the  $d$  bands are given in Figure 3. In all the free energy surfaces, the valley near  $q = -1$  corresponds to a solvated proton close to the metal surface; the minimum near  $q = 0$  represents the adsorbed hydrogen atom. The two minima are separated by a barrier with a saddle point of  $\Delta G_{\text{act}}$  height.

In accord with experimental findings, the activation barrier is highest for Cd, because its  $d$  band lies well below the Fermi level to affect the activation energy; therefore it has no catalytic effect and the reaction is mostly dominated by the  $sp$  band. On the coin metals Cu, Ag, and Au, the reaction has the same activation energies. This is due to a compensation effect: the interaction with the  $d$  band increases down the column of the periodic table, which lowers the energy of

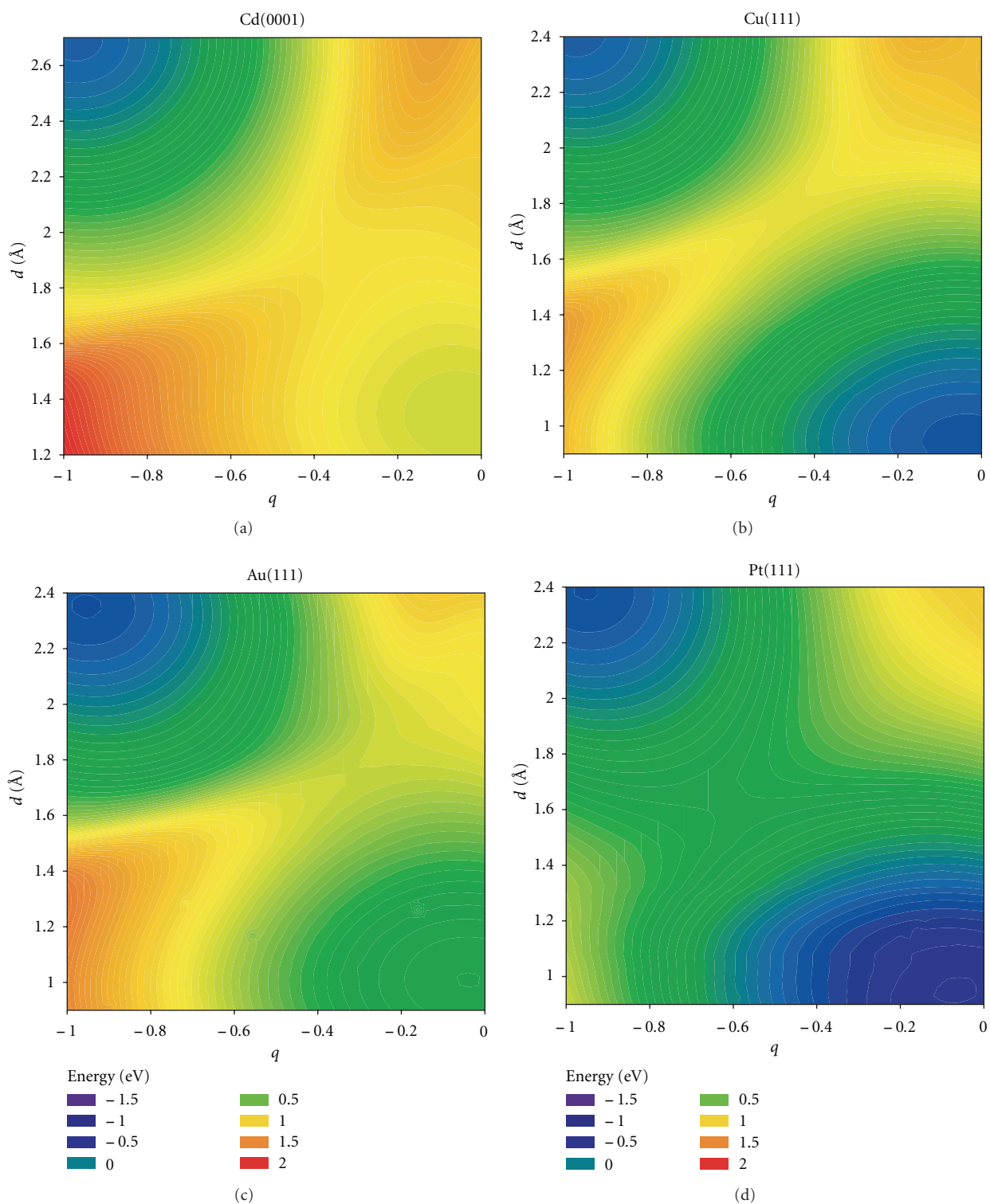


FIGURE 2: Free energy surfaces for hydrogen adsorption at Cd(0001), Cu(111), Au(111), and Pt(111).

activation. On the other hand, the energy of the adsorbed hydrogen increases in the same order therefore; the reaction free energy for the adsorption rises, which in turn raises the activation energy. On all the three coin metals, the  $d$  band lies well below the Fermi level and both the bonding and

the antibonding parts of the hydrogen DOS caused by the interaction with the  $d$  band are filled, so that the  $d$  band does not contribute much to the adsorption bond which is dominated by the interaction with the  $sp$  band. Of all the metals considered, Pt is the only one whose  $d$  band extends

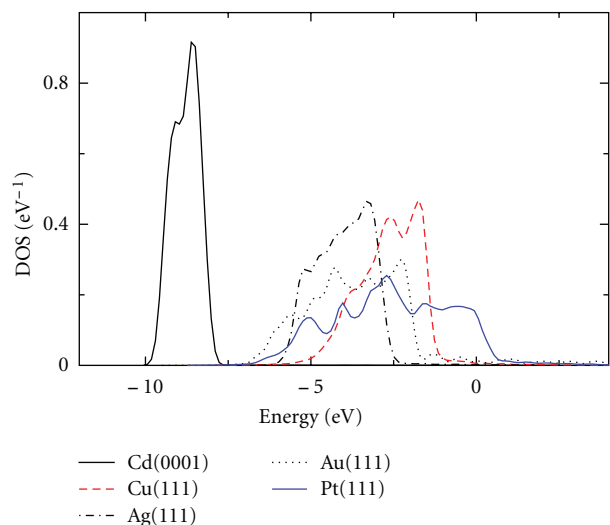


FIGURE 3: Surface  $d$  band DOS of the metals considered. The Fermi level has been taken as the energy zero.

over the Fermi level. Its interaction with H is strong, and therefore, it has by far the lowest activation energy. At the equilibrium electrode potential, the energy of the adsorbed hydrogen is lower than that of the solvated proton. Therefore, adsorption sets in at potentials above the hydrogen evolution, so that one speaks of strongly adsorbed hydrogen ( $H_{\text{upd}}$ ). However, there is convincing experimental evidence that this is not the species that takes part in hydrogen evolution [12], but the intermediate is a more weakly adsorbed species. So, our calculations correspond to the deposition of strongly adsorbed hydrogen. Experimentally, this reaction is so fast that it has not been possible to measure its rate. This is in line with the very low energy of activation that we reported.

So far, we have shown that explicit model calculations performed for the densest crystal surfaces reproduced well the observed experimental trends and, even, gave a good estimate for the reaction rates [11, 13], but for long time, it has been known that the rate of hydrogen evolution depends strongly on the electrode material. When well-defined single-crystal electrodes became available, an important question was whether the rate depends only on the nature of the electrode or on the crystal face as well. Experiments on silver [14, 15] and copper [16] showed that, in both cases, the (111) surface was the better catalyst. The differences in the rate constants between various facets of Ag and Cu are not large and, as yet, unexplained. Hence, we have also investigated the hydrogen evolution on silver and copper on open crystal faces, such as (100) surfaces, and compared our results with the (111) surfaces [17].

To begin with, we have calculated the free energies of adsorption of hydrogen on the four surfaces that we consider. On both metals, the adsorption energy is less favourable on the (100) than on the (111) surface (Table 2) and the lowest energy is associated with the four- and threefold hollow sites, respectively.

To understand the effect of the metal  $d$  band on the H-metal bond, an analysis of the surface  $d$  band DOS is

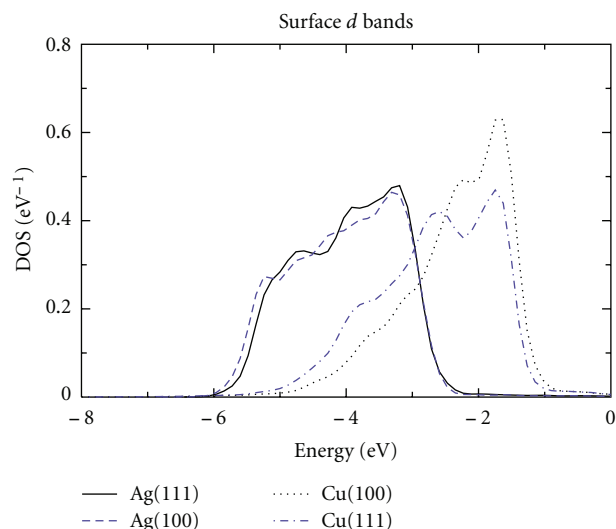


FIGURE 4: Surface density of states of the  $d$  bands. The Fermi level has been taken as the energy zero.

TABLE 2: Reaction free energy and free energy of activation for the Volmer reaction on the hydrogen scale [17].

Metal	Ag(111)	Ag(100)	Cu(111)	Cu(100)
$\Delta G_{\text{ad}}$ (eV)	0.39	0.48	0.10	0.14
$\Delta G_{\text{act}}$ (eV)	0.71	0.81	0.71	0.79

helpful. Figure 4 shows the  $d$  band structure for each system. As it can be seen, all the  $d$  bands lie below the Fermi level indicating that they are mediocre catalysts. The hydrogen-metal interaction splits the  $1s$  hydrogen orbital in a bonding and an antibonding part. Since both parts are located well below the Fermi level, they are filled and no bonding results. Thus, the hydrogen adsorption is purely due to the hydrogen- $sp$  band interaction. Because silver and copper  $d$  bands are filled and they do not contribute to the bonding, the Pauli repulsion becomes important, probably inducing a weaker adsorption on these open surfaces.

In the framework of our theory, we have investigated the Volmer reaction (the first step in hydrogen evolution) as described in [11, 17]. The resulting free energy surfaces for a variable energy of reorganization  $\lambda$  and the standard hydrogen potential are shown in Figure 5. In all the surfaces, the minimum the upper left corner, at  $q = 1$ , corresponds to the initial state, the solvated proton, and the minimum at the bottom right corner,  $q = 0$ , to the final state, the adsorbed hydrogen atom. In all cases the final state has higher free energies, which are the values given in Table 2. These two states are separated by an energy barrier; the energy of the saddle point gives the free energy of activation of the Volmer reaction, which is also given in the table. For both metals, the energy of activation is higher for the surface with the higher free energy of adsorption, as may have been expected. Thus, in agreement with experimental data, we find higher activation energies and, hence, lower rate constants, for the (100) than for the (111) surfaces. The main cause is the

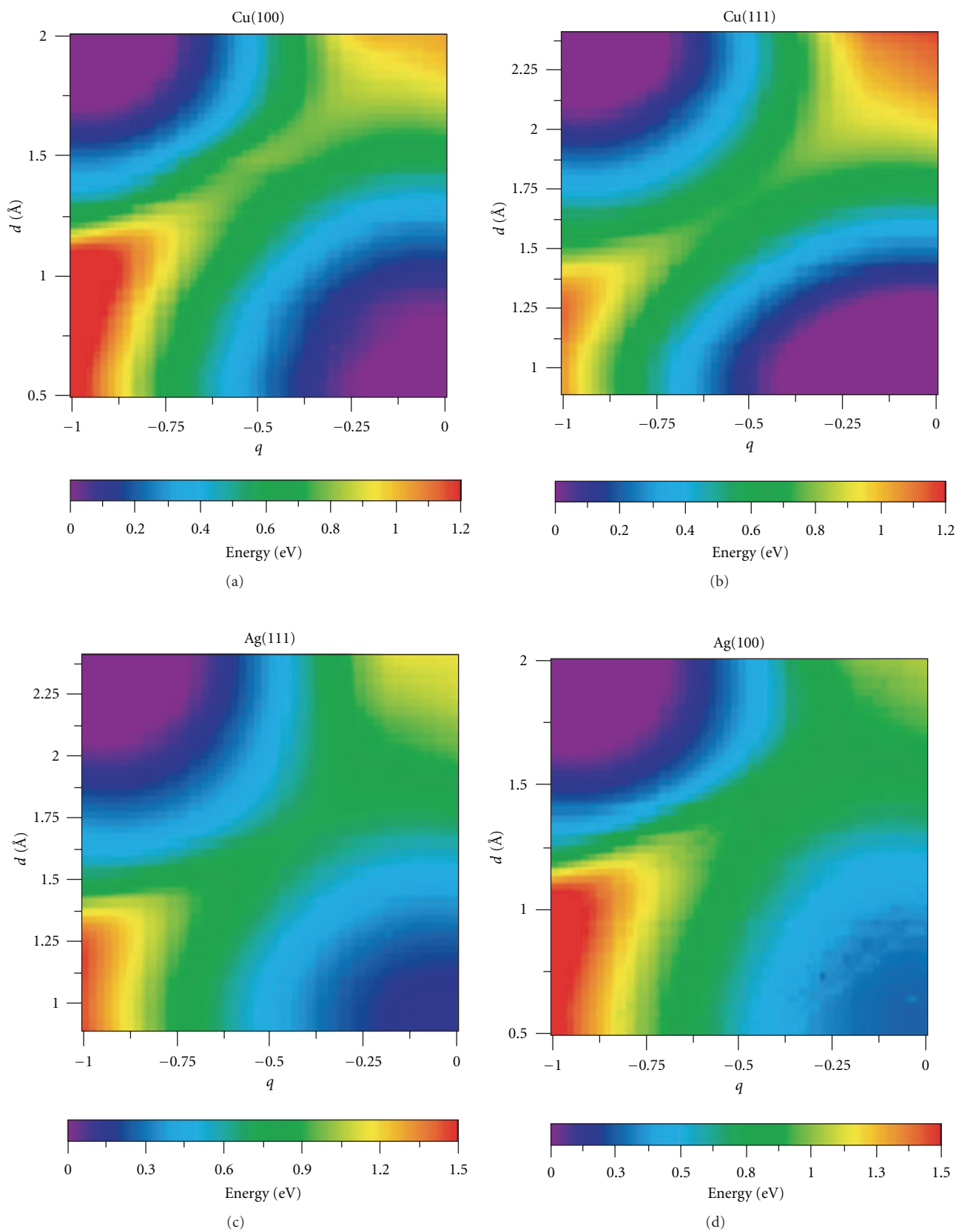


FIGURE 5: Free energy surfaces for hydrogen adsorption on single-crystal surfaces of copper and silver.

more endergonic adsorption energy on the open surfaces. For silver, both theory and experiments [14] suggest that the second step is the electrochemical desorption of the hydrogen atoms. On copper, the same mechanism is likely to operate, though we cannot rule out at what low absolute values of the overpotential chemical recombination may occur. Thus, electrochemical desorption seems to be more prevalent than previously thought [12, 18], and there is a need for a theoretical description of this process. Corresponding work is in progress in our group.

## 4. Electrocatalytic Properties of Nanostructures

**4.1. Intrinsic Chemical Nature and Strain Effect: Monolayers of Pd on (111) Substrates.** Electrochemical nanostructures have gained a great interest in the last decade because of the large variation of their reactivity in comparison with bulk material [19–25]. An interesting aspect is the possibility to design at the nano scale materials with specific properties in order to improve the electrocatalytic properties of electrodes. In this sense, electrochemistry offers convenient techniques for the synthesis of nanostructures such as metal overlayers, steps decorated by adatoms, or even monoatomic nanowires [26, 27]. One of the main features of nanomaterials is that their properties can be controlled by their electrochemical potential, a variable that is not available in vacuum or in air. This makes electrochemical nanostructures versatile. The big scientific challenge is to understand how the structure affects the chemical and physical properties of the materials and how this in turn influences their reactivity [28]. However, the implementation of these nanostructures is difficult because of the lack of understanding of the fundamental aspects and mechanisms which determine their stability, reactivity, and dynamics.

In the framework of our theory, we have examined the reactivity of various nanostructures on which much attention has been focused recently. Particularly, the role of the geometry and chemistry of the substrate on the electrocatalytic activity was investigated.

Monolayers of foreign atoms deposited on different metallic substrates have been extensively studied from an experimental point of view. We have systematically investigated monolayers of Pd at different substrates  $M(111)$ ,  $M = \text{Pt, Au, Ni, Cu, Ru, Pd}$ .

Figure 6 shows the contour plots of the potential energy surfaces calculated by employing parameters which correspond to the hydrogen oxidation reaction. To analyse the catalytic activity of the systems, we focus on the region corresponding to the transition state, where the bond of the molecule starts to break and the electrons are being transferred to the electrode. In accord with experiments [19–21], a monolayer of Pd on Au(111) shows the best catalytic property, while the activity of the deposit on Cu(111) is the lowest. All the cases are compared with Pd(111). Pd on Ru(111) shows a similar behaviour as Pd on Cu(111), while Pd on Pt(111) is slightly less active than Pd(111).

As we explained in detail [29], there exists different factors which can affect the reaction. Frequently, these changes on the catalytic reactivity are explained in terms of

strains in the lattice of the deposited monolayer resulting in a shift of the  $d$  band center to higher or lower energies. Since the overlap of metal  $d$  states at neighbouring sites is affected, the band width is also simultaneously modified. Thus, the interaction with the reactants also changes [30].

We have systematically studied a palladium monolayer at different substrates having either larger or smaller lattice constants ( $a_0$ ). Figure 7 illustrates the strain effect mentioned above for two extreme cases: when Pd is deposited on Au(111), the monolayer is expanded with respect to the bulk Pd ( $a_0^{\text{Pd}} < a_0^{\text{Au}}$ ), consequently the distance between nearest neighbours increases. In contrast, when it is deposited on Cu(111), it is compressed ( $a_0^{\text{Pd}} > a_0^{\text{Cu}}$ ) and the distortions produce changes in the electronic properties.

Particularly, the density of states of the  $d$  band shows important alterations. However, these changes are too complex to be explained only by a modification of the geometrical arrangements. Specific chemical interactions between the substrate and the monolayer should also play an important role.

To clarify the strain effect and the influence of the substrate on the reactivity, a set of theoretical systems have been investigated by us [29]. We have replaced the value of the lattice constant of Pd by that corresponding to the different substrates employed for the deposit and calculated the density of states for the surface of Pd(111) with this fixed value. Obviously, these are not *real* systems but their electronic behaviors allow us to distinguish between the strain effect and the role played by the chemical interactions between the foreign atom and the substrate. Figure 8 shows the comparison of the electronic properties, specifically on the shapes and position of the  $d$  bands. The lattice constants decrease from top to bottom. The distribution of electronic states for the bare (111) surfaces of the different substrates is shown on Figure 8(a). Here, the effect of the lattice constant does not produce a systematic change because of other effects that are also involved. There exists a combination of two factors: going from left to right in the periodic table, the number of  $d$  electrons increases, and thus the position of the  $d$  band relative to the Fermi level shifts to lower energies, and going from top to bottom the orbitals are more extended in space producing a higher overlap, and thus the bands are wider.

The effect of the lattice constant can be observed in the middle part of Figure 8(b) for the *artificial* systems obtained for Pd(111) with the lattice constants of the other metals. Here, the number of electrons is constant and the spatial extension of the orbitals is the same. When the lattice constant decreases, the delocalization of the orbitals increases producing the extension of the  $d$  band into lower energies. The distribution of the electronic states of the  $d$  band of a monolayer of Pd deposited on different substrates is shown on the right side of Figure 8(c). Here, the structure of the  $d$  band is the result of the combination of all the effects mentioned above. In general, one observes a widening of the  $d$  band with the decrease of the lattice constant of the substrate, whose orbitals are located at different energies depending on its chemical nature (see Figure 8(a)). The density of states decreases slightly at the Fermi level in all the cases, but it appears to be more localized at lower energies.

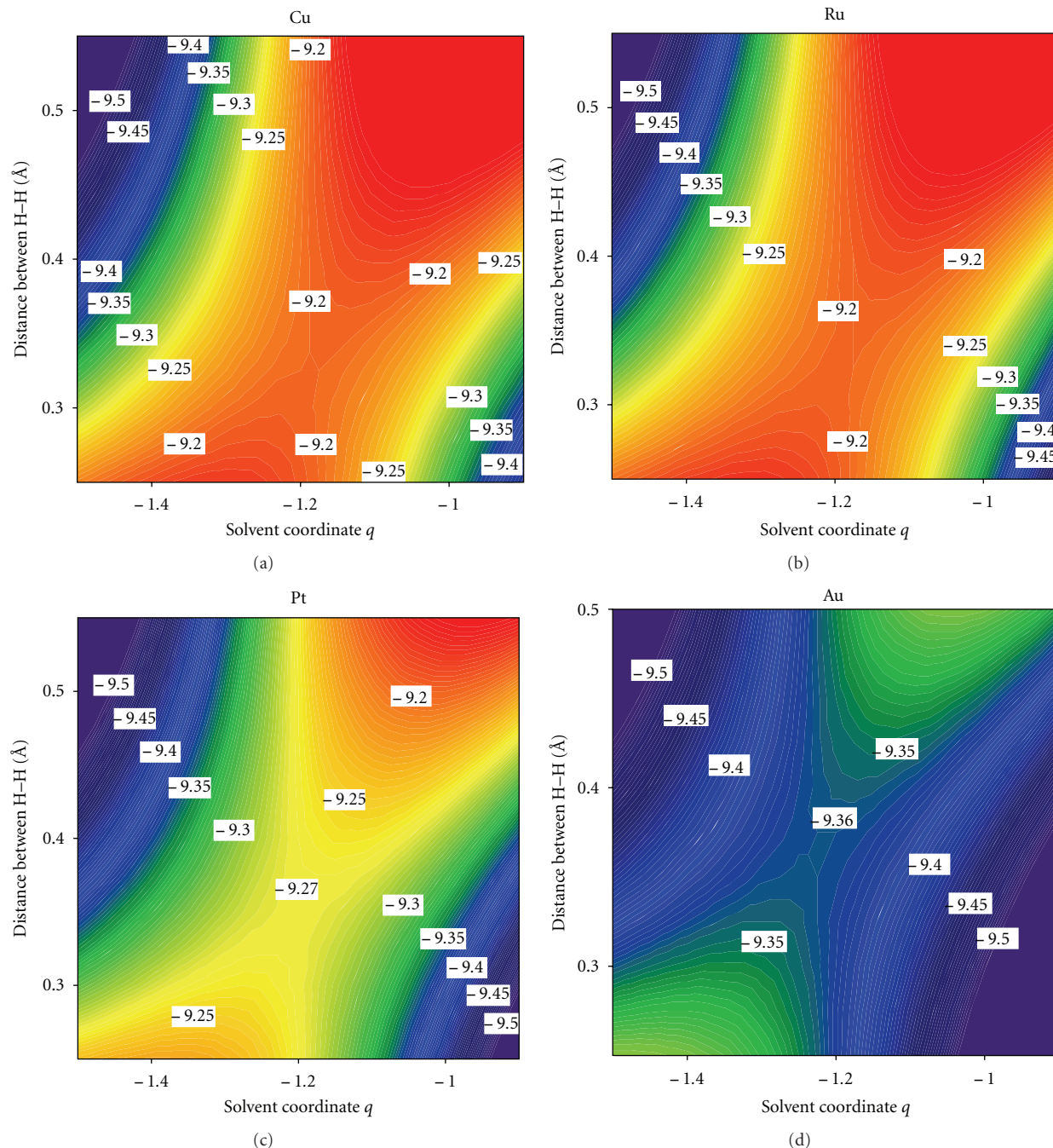


FIGURE 6: Contour plots of the potential energy surfaces showing the saddle point of the reaction path for the hydrogen oxidation at a monolayer of Pd deposited on different substrates M(111). The projections are done on the plane of the solvent coordinate  $q$  and the distance between both hydrogen atoms relative to the equilibrium in the molecule.

This effect is especially noticeable by the monolayer of Pd deposited on Au(111), where a sharp peak is observed at about  $-0.5$  eV below the Fermi level.

Thus, in order to predict the catalytic activities of these systems, it is not enough to make estimations considering the strain produced by the different lattice constants of the substrates; it is necessary to make a more detailed analysis taking into account specific chemical interactions with the substrate.

*4.2. Intrinsic Chemical Nature and Geometrical Effect: Noble Metal Nanowires Supported on Graphite Edges.* Due to their unique properties, nanowires are employed in many applications and electrochemistry is one of them. In a recent communication, we have investigated the catalytic properties of isolated monoatomic wires. Cu and Au free-standing wires were predicted to be promising catalysts for the hydrogen reaction [31]. However, it is known that isolated wires are impractical as electrocatalysts. Therefore, we focus in more

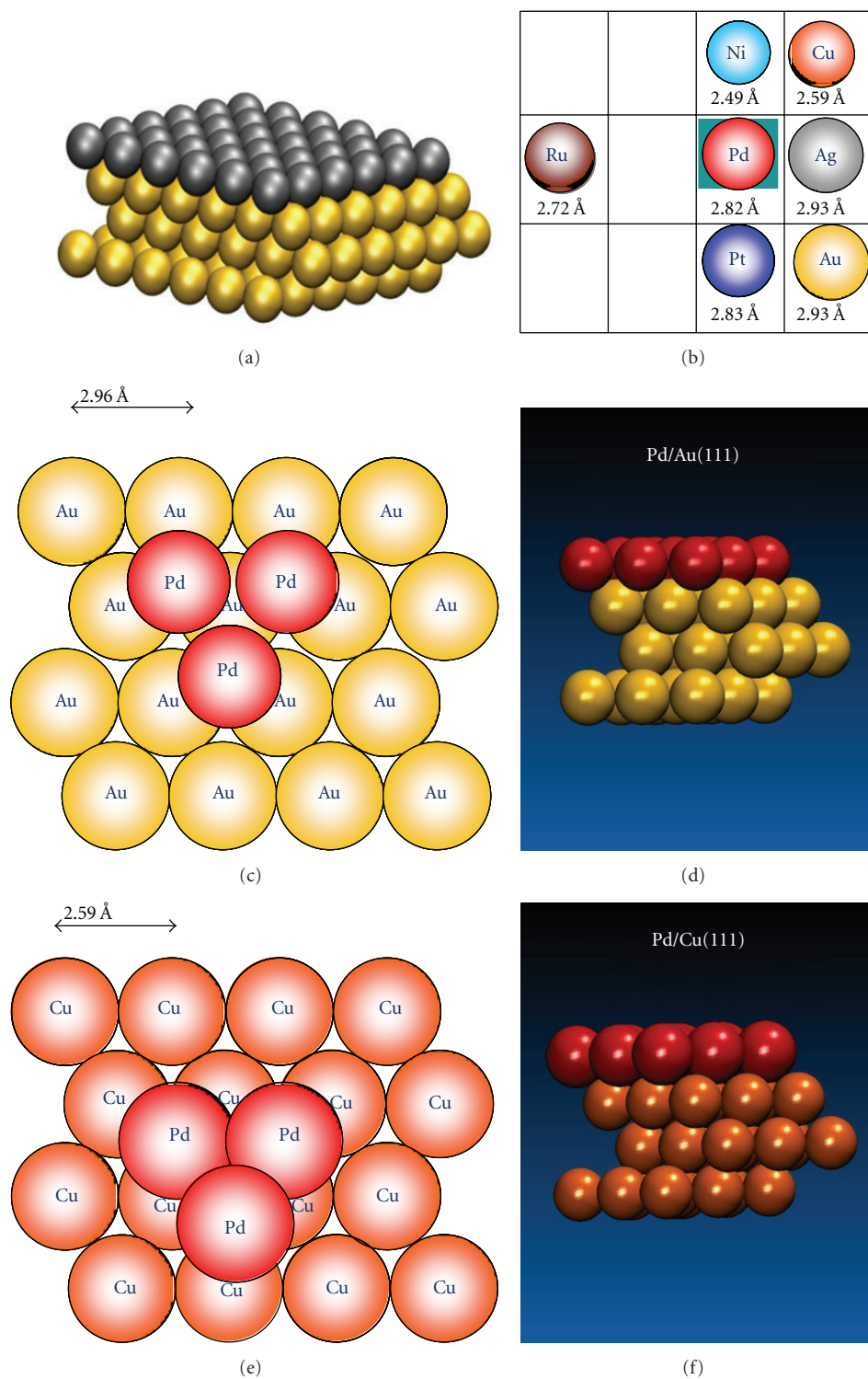


FIGURE 7: Monolayer of Pd on different substrates: M(111) (a). Distances to the next neighbours for the different substrates in comparison with Pd bulk (b). Expanded (c, d) and compressed (e, f) structures of the monolayer when the substrate atoms are larger and smaller than Pd, respectively.



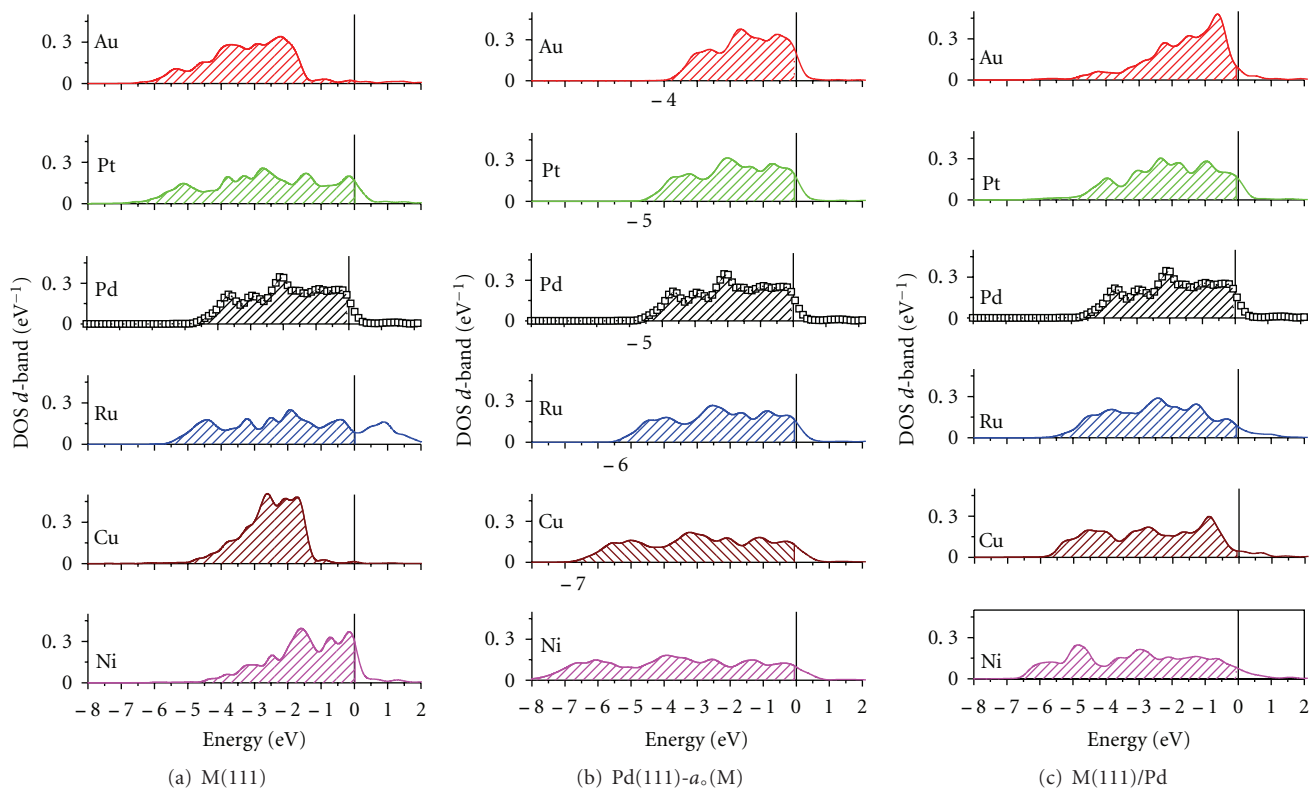


FIGURE 8: Density of states projected on the  $d$  bands for three different systems: (a) atoms at the surface (111) for different metals  $M$ , (b) atoms at the surface of Pd(111), where the lattice constant  $a_0$  of palladium has been *artificially* changed by that of different metals  $M$ ; (c) atoms of the monolayer of Pd deposited on different metallic substrates  $M(111)$ . The vertical lines indicate the position of the Fermi level.

realistic systems, where these nanowires are supported on inert substrates to examine their stability and the influence of their chemical properties on the electrocatalytic activity (for details, see [32]).

Specifically, we considered Pt and Au monoatomic wires attached to monoatomic steps on the basal planes of graphite, the so-called graphite-supported wires (GSW). Considering the  $sp^2$  hybridization of the carbon orbitals and the distance between two unsaturated carbon atoms (2.46 Å), which fits quite well the bond distances of the bare wires ( $\approx 2.50$  Å), the zigzag arrangement was taken as the initial configuration. The system is shown in Figure 9—more detailed information can be found in [32].

The chain of metal atoms shows a corrugation along the  $z$ -axis forming an angle  $\theta$ , which, in these commensurate structures is induced by the graphite lattice. The binding energy of the systems per metal atom is given in Table 4.

As it can be concluded from the adsorption energies, both metals adsorb exothermically, but the wire-graphite bond is much stronger for Pt. This fact can be revealed by a detailed analysis of the projected density of states (PDOS) of the orbitals involved in the graphite-wire bond (Figure 10).

In the systems under study, the overlapping orbitals are  $sp_y^2$  of the carbon atoms  $C_{\text{edge}}$  and  $d_{x^2-y^2}$  of each metal. Before the adsorption process,  $sp_y^2$  of  $C_{\text{edge}}$  is centered at the Fermi level;  $d_{x^2-y^2}$  of the metals is below the Fermi level in Au-GSW and above it in Pt-GSW. During the

adsorption process,  $sp_y^2$  of  $C_{\text{edge}}$  and  $d_{x^2-y^2}$  of the metals overlaps and splits into a bonding and an antibonding parts. The bonding contribution appears below the Fermi level for both metals (Figure 10). The antibonding contribution is below the Fermi level only in Au-GSW, and this is the reason for the differences in the binding energy: the binding of Pt on graphite is stronger because the antibonding is unoccupied.

In the search for a good electrocatalyst for the hydrogen reaction, the hydrogen-GSWs adsorption was also investigated. The hydrogen adsorption process can occur on the attached wires at several positions and also directly on the graphite, cleaving one wire-graphite bond. Both situations were considered, and the most stable configurations for the adsorption are shown in Figure 11 together with their energies of adsorption.

To clarify the behavior of these systems, we must analyze the bond formation and the adsorption energies of hydrogen (Table 4). In Figure 12, the DOSs of the metal states overlapping with hydrogen are plotted and compared with the same orbitals in the absence of hydrogen. The adsorbate overlaps not only with  $d$  but with  $p$  states. On surfaces,  $p$  orbitals form a wide band spanning the Fermi level; this delocalization of the  $p$  band occurs on all metals.

In BW and GSW, only the  $p$  orbital along the axis of the wire is delocalized ( $p_x$  in our case) and the others are empty.  $p_y$  is empty in GSW; therefore, its DOS appears above the Fermi level for Au and Pt (In Figure 12, top). However,

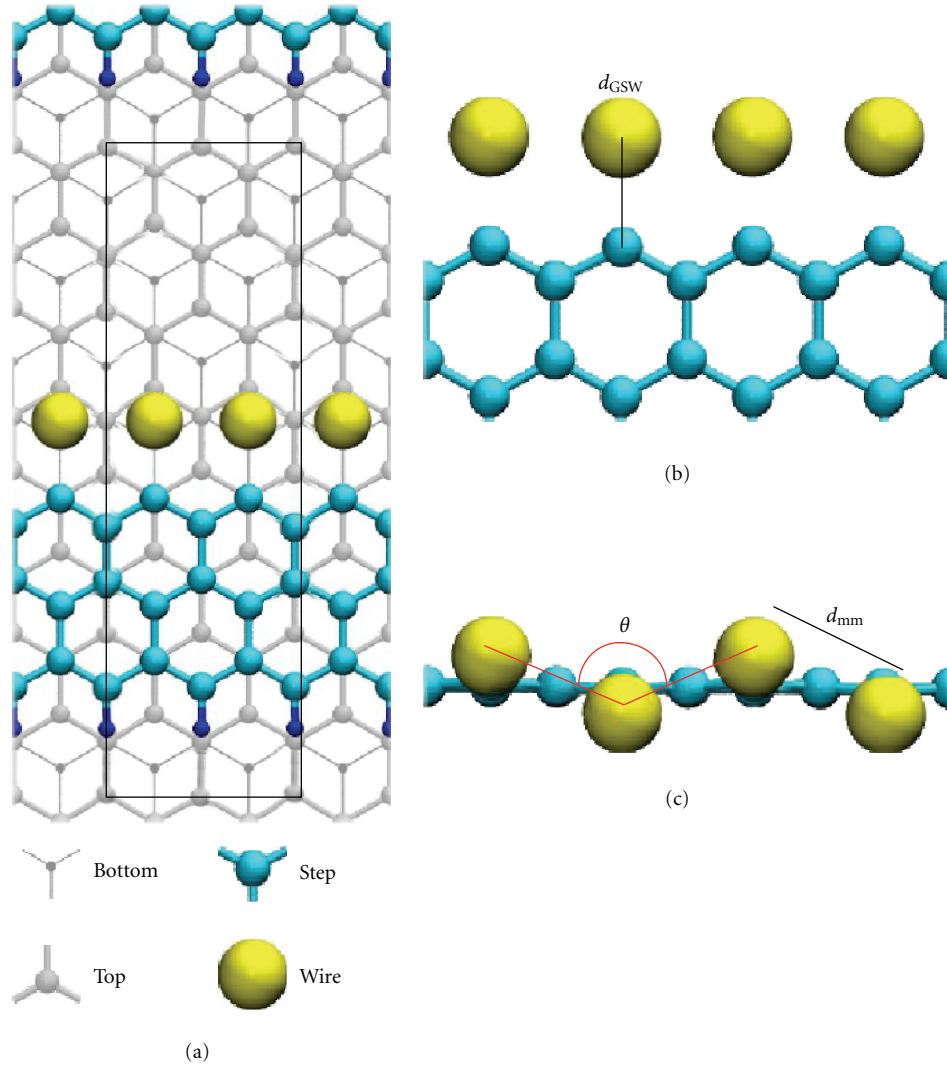


FIGURE 9: (a) The system (GSW—graphite supported wires) is formed by two layers (black and cyan), one step (blue), and the wire (yellow). The unit cell is indicated with red dash lines. (b) Metal-metal distance ( $d_{\text{GSW}}$ ). (c) Corrugation angle of the wire ( $\theta$ ).

TABLE 3: Binding energy ( $E_{\text{bin}}$ ), wire-graphite bond distance ( $d_{\text{GSW}}$ ), metal-metal distance of bare wire ( $d_{\text{mm(BW)}}$ ) and graphite-supported wires ( $d_{\text{mm(GSW)}}$ ), the zigzag angle ( $\theta$ ) is shown in Figure 9(c).

Wires	$E_{\text{bin}}$ (eV)	$d_{\text{GSW}}$ (Å)	$d_{\text{mm(GSW)}}$ (Å)	$d_{\text{mm(BW)}}$ (Å)	$\theta$ (°)
Au	-1.78	2.08	2.68	2.61	133.2
Pt	-3.29	1.95	2.54	2.39	151.1

TABLE 4: Hydrogen adsorption energies on fcc(111) surfaces, bare wires [31] and wires of GSW.

$E_{\text{ads}}$ (eV)	Au	Pt
fcc(111)	0.17	-0.49
BW	-0.751	-0.573
GSW	-0.548	0.055

after the adsorption of hydrogen, the  $p_y$  of both metals lie below the Fermi level and strongly overlap with hydrogen. Besides the overlap with  $p_y$ , hydrogen overlaps with  $d$  states:

for geometric reasons, with  $d_{z^2}$  in the case of Pt and with  $d_{x^2-y^2}$  in the case of Au.  $p_y$  and  $d_{z^2}$  in platinum wire have almost the same profile, which indicates a hybridization between these two states; the resulting orbital overlaps with hydrogen. In contrast,  $p_y$  and  $d_{x^2-y^2}$  of gold overlap separately with hydrogen. As can be noticed, hydrogen bonds similarly on both metals. The difference in the adsorption energies is because Au-GSW is more reactive than Pt-GSW due to the Au-graphite weaker bond.

As mention previously, the adsorption of hydrogen on graphite was also studied. In this case, the adsorption energy is lower than on wires for Au-GSW but almost the same for

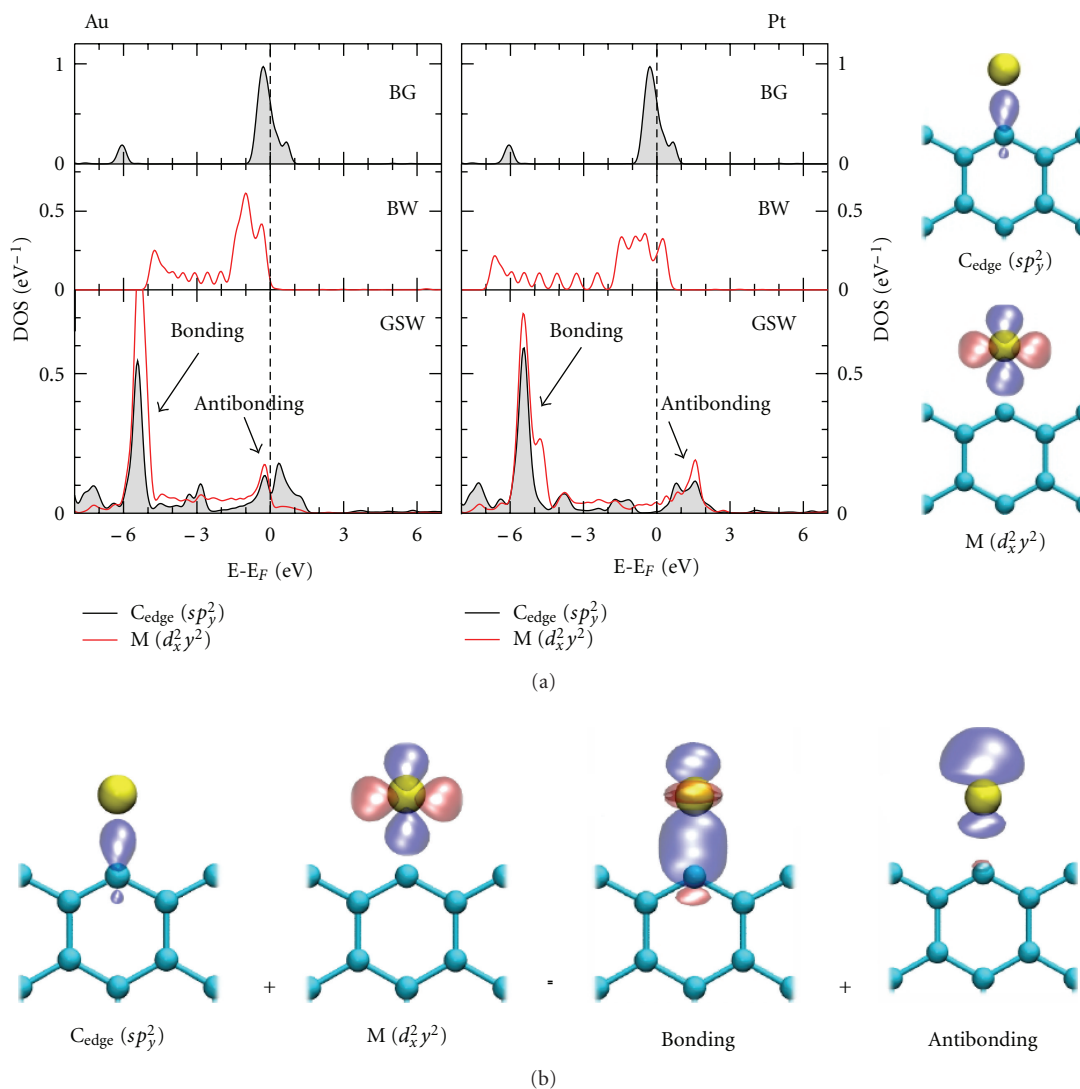


FIGURE 10: (a) PDOS of the  $sp_y^2$  of  $C_{\text{edge}}$  and the  $d_{x^2-y^2}$  of the metal for BG (bare graphite), BWs (bare wires) and GSWs (graphite supported wires) of gold and platinum. (b) Bonding and antibonding orbitals of the wire-graphite bond. The antibonding orbital is occupied only in the case of Au.

Pt-GSW (Figure 11). A cleavage of the wire-graphite bond is observed on Au-GSW, and a single bond of hydrogen with  $C_{\text{edge}}$  is formed. However, in the case of Pt-GSW, the adsorption process does not imply bond breaking and a simple bond with  $C_{\text{edge}}$  is formed. These results suggest that in the presence of hydrogen, gold wires may desorb from graphite, which may not be the case for platinum.

On the platinum wires, hydrogen adsorption is isoenergetic, because the platinum-graphite bond is weakened. However, hydrogen adsorption on the wire and on graphite is almost the same, and it does not imply desorption of the wire. Finally, hydrogen adsorption on the supported gold wires is more favorable than at Au(111) surfaces, and at 0 V SHE and pH 0, such a gold wire would be covered with a layer of strongly adsorbed hydrogen. Thus, these wires also promise to be good catalysts, just like the bare gold wires, but for a definite conclusion, more studies are needed.

## 5. Outlook

The results presented in this paper have been mostly oriented to investigate the hydrogen reaction on pure single-crystal surfaces and monolayers of a foreign metal on a variety of (111) substrates, in good agreement with experimental data reported in the literature. In addition and to the best of our knowledge, this is the first explanation of the hydrogen electrocatalysis founded on a theory and not on a correlation.

In the last few years, the searching for a better catalyst was centered on pure and modified single-crystals. However, the hope for the future advances in electrochemistry focuses no longer on such surfaces but on nanostructures, due to the fact that they are cheaper, more versatile, and efficient [33].

Dealing with nanomaterials is a challenge for both experiments and theory. Hence, our goal is to combine DFT and our theory to elucidate the electronic structure and predict

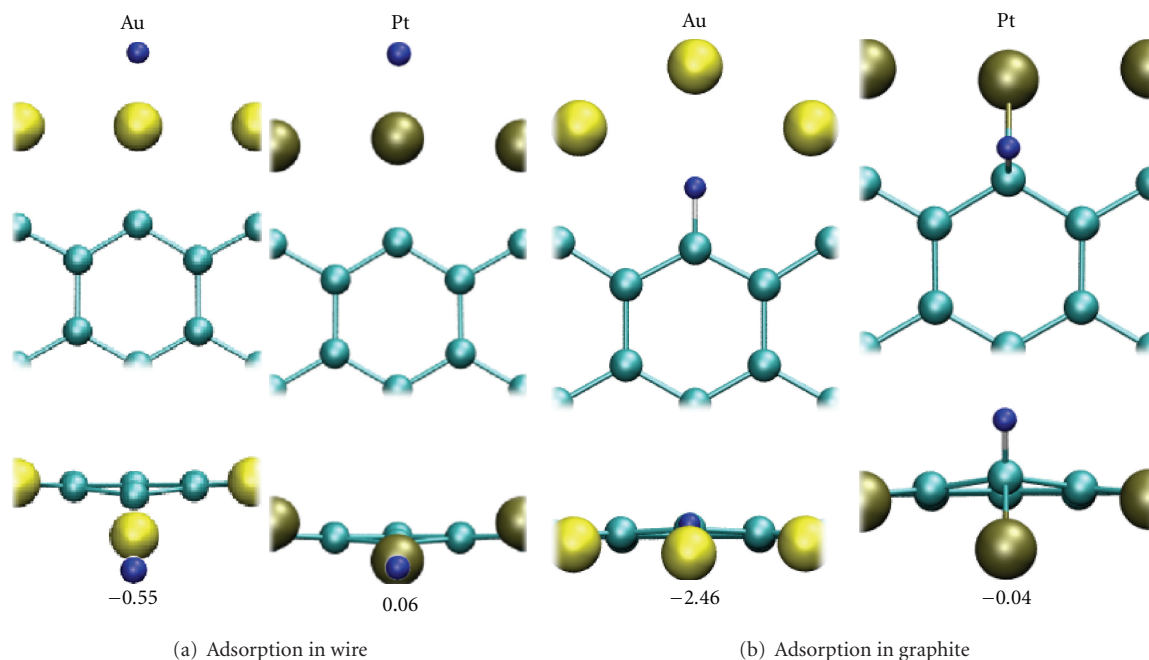


FIGURE 11: Configuration of the most stable adsorption of hydrogen (blue) on the wire (a) and at the edge of graphite (b) of GSW. The corresponding energies in eV are shown below. On the wire, for both metals, the adsorption is on top. On the graphite edge, the adsorption is in the same plane in the case of gold and above it in the case of platinum.

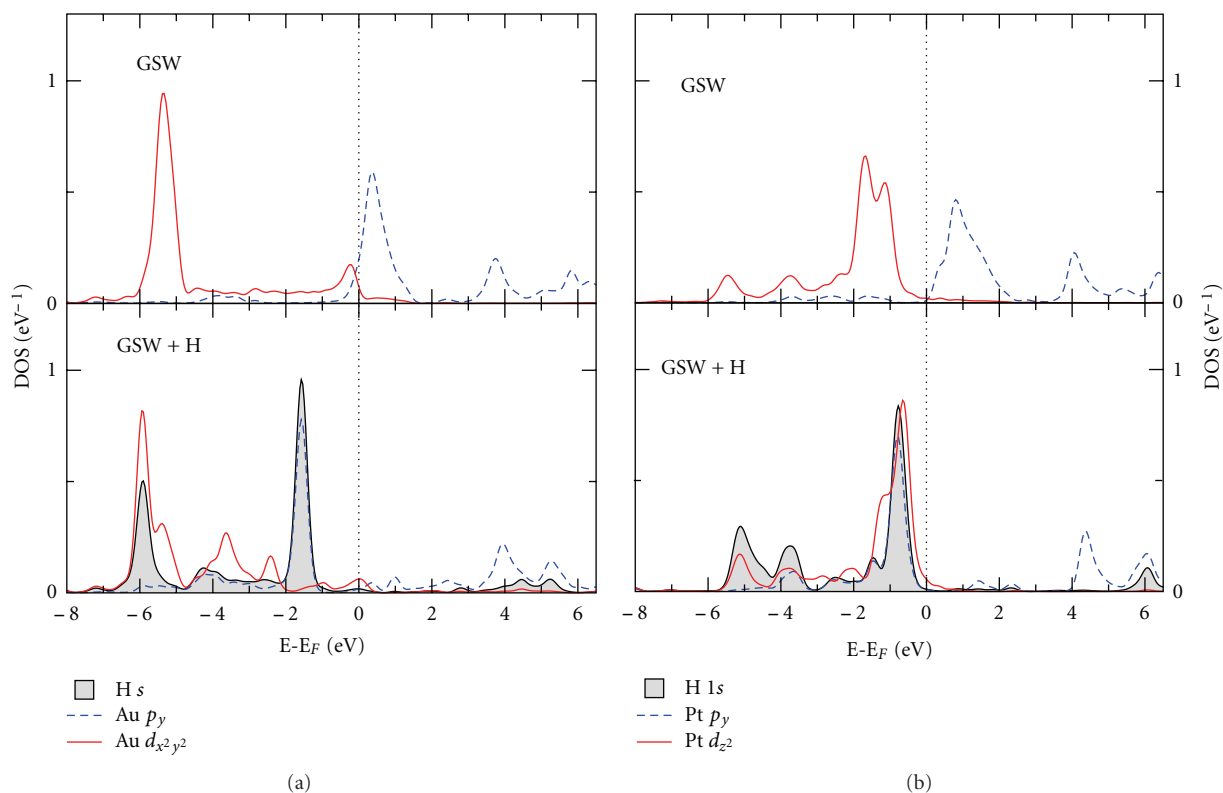


FIGURE 12: DOS of  $d_{x^2-y^2}$  and  $p_y$  of the metals for Au-GSW;  $d_{z^2}$  and  $p_y$  for Pt-GSW with and without H.  $p_y$  of the metals is empty in the absence of hydrogen, and becomes occupied when hydrogen adsorbs.

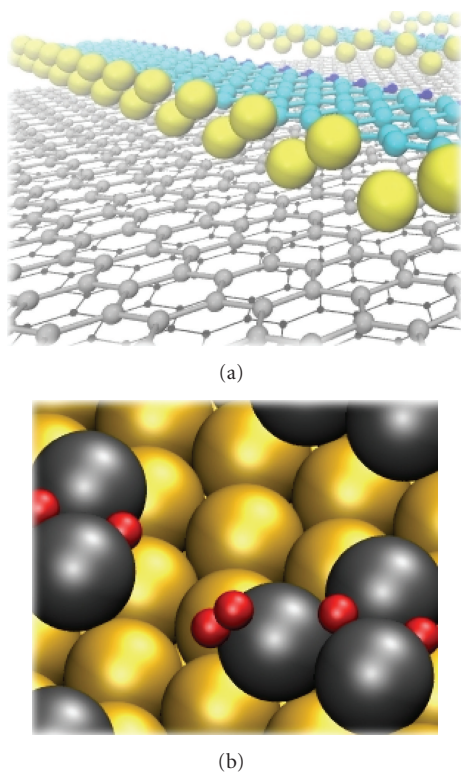


FIGURE 13: (a) Wire Adsorption on Graphite steps. (b) Hydrogen adsorption on Pd nanoclusters on Au(111).

their catalytic activity. In this context, Pd submonolayers on Au substrates and graphite-supported wires (Figure 13) are being investigated in our group.

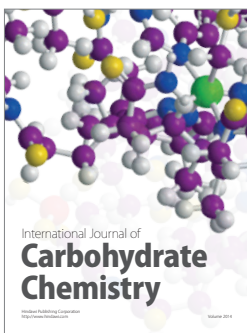
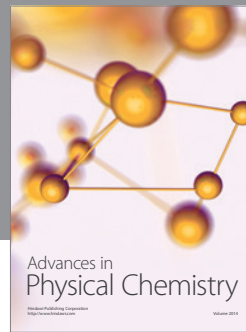
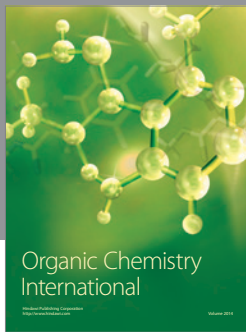
## Acknowledgments

Financial support by the Deutsche Forschungsgemeinschaft under Schm 344/40-1, Sa 1770-1,2 and FOR1376, Mincyt-BMBF, CONICET, the European Union under ELCAT, PICT-2008-0737 (ANPCyT), and a generous grant of computing time from the Baden-Württemberg grid is gratefully acknowledged. E. Santos, P. Quaino, W. Schmickler thank CONICET for continued support.

## References

- [1] E. Santos and W. Schmickler, "d-band catalysis in electrochemistry," *ChemPhysChem*, vol. 7, no. 11, pp. 2282–2285, 2006.
- [2] E. Santos and W. Schmickler, "Fundamental aspects of electrocatalysis," *Chemical Physics*, vol. 332, no. 1, pp. 39–47, 2007.
- [3] E. Santos, M. T. M. Koper, and W. Schmickler, "A model for bond-breaking electron transfer at metal electrodes," *Chemical Physics Letters*, vol. 419, no. 4–6, pp. 421–425, 2006.
- [4] E. Santos, M. T. M. Koper, and W. Schmickler, "Bond-breaking electron transfer of diatomic reactants at metal electrodes," *Chemical Physics*, vol. 344, no. 1-2, pp. 195–201, 2008.
- [5] P. W. Anderson and A. T. Ramsey, "Localized magnetic states in metals," *Physical Review*, vol. 124, p. 41, 1961.
- [6] D. M. Newns, "Self-consistent model of hydrogen chemisorption," *Physical Review*, vol. 178, no. 3, pp. 1123–1135, 1969.
- [7] E. Santos and W. Schmickler, "Electrocatalysis of hydrogen oxidation—theoretical foundations," *Angewandte Chemie*, vol. 46, no. 43, pp. 8262–8265, 2007.
- [8] E. Santos, K. Pötting, and W. Schmickler, "On the catalysis of the hydrogen oxidation," *Faraday Discussions*, vol. 140, pp. 209–218, 2008.
- [9] E. Santos and W. Schmickler, "Electronic interactions decreasing the activation barrier for the hydrogen electro-oxidation reaction," *Electrochimica Acta*, vol. 53, no. 21, pp. 6149–6156, 2008.
- [10] E. Santos, A. Lundin, K. Pötting, P. Quaino, and W. Schmickler, "Hydrogen evolution and oxidation—a prototype for an electrocatalytic reaction," *Journal of Solid State Electrochemistry*, vol. 13, no. 7, pp. 1101–1109, 2009.
- [11] E. Santos, A. Lundin, K. Pötting, P. Quaino, and W. Schmickler, "Model for the electrocatalysis of hydrogen evolution," *Physical Review B*, vol. 79, no. 23, Article ID 235436, 2009.
- [12] E. Santos and W. Schmickler, *Interfacial Electrochemistry*, Springer, London, UK, 2nd edition, 2010.
- [13] E. Santos and W. Schmickler, *Electrocatalysis; From Fundamental Aspects to Fuel Cells*, 2010.
- [14] D. Eberhardt, E. Santos, and W. Schmickler, "Hydrogen evolution on silver single crystal electrodes—first results," *Journal of Electroanalytical Chemistry*, vol. 461, no. 1-2, pp. 76–79, 1999.
- [15] L. M. Doubova and S. Trasatti, "Effect of the crystallographic orientation of Ag single crystal face electrodes on the kinetics of proton discharge," *Journal of Electroanalytical Chemistry*, vol. 467, no. 1, pp. 164–176, 1999.
- [16] V. V. Batrakov, Y. Dittrikh, and A. N. Popov, "Influence of the surface structure on the overpotential for hydrogen evolution in acid solutions," *Elektrokhimiya*, vol. 8, p. 640, 1972.
- [17] E. Santos, K. Pötting, A. Lundin, P. Quaino, and W. Schmickler, "Hydrogen evolution on single-crystal copper and silver: a theoretical study," *ChemPhysChem*, vol. 11, no. 7, pp. 1491–1495, 2010.
- [18] W. Vielstich, C. H. Hamann, and A. Hamnett, *Electrochemistry*, Wiley-VCH, Cambridge, UK, 2007.
- [19] S. Pandelov and U. Stimming, "Reactivity of monolayers and nano-islands of palladium on Au(1 1 1) with respect to proton reduction," *Electrochimica Acta*, vol. 52, no. 18, pp. 5548–5555, 2007.
- [20] H. Wolfschmidt, R. Bussar, and U. Stimming, "Charge transfer reactions at nanostructured Au(111) surfaces: influence of the substrate material on electrocatalytic activity," *Journal of Physics Condensed Matter*, vol. 20, no. 37, Article ID 374127, 2008.
- [21] L. A. Kibler, "Hydrogen electrocatalysis," *ChemPhysChem*, vol. 7, no. 5, pp. 985–991, 2006.
- [22] F. Hernandez and H. Baltruschat, "Hydrogen evolution and Cu UPD at stepped gold single crystals modified with Pd," *Journal of Solid State Electrochemistry*, vol. 11, no. 7, pp. 877–885, 2007.
- [23] H. Baltruschat, R. Bussar, S. Ernst, and F. Hernandez, *In-Situ Spectroscopic Studies of Adsorption at the Electrode and Electrocatalysis*, Elsevier, 2007.
- [24] R. R. Adzic, A. V. Tripkovic, and V. B. Vessovic, "Structural effects in electrocatalysis: oxidation of formic acid and hydrogen adsorption on platinum single-crystal stepped surfaces," *Journal of Electroanalytical Chemistry*, vol. 204, no. 1-2, pp. 329–341, 1986.

- [25] G. Garcia and M. T. M. Koper, "Stripping voltammetry of carbon monoxide oxidation on stepped platinum single-crystal electrodes in alkaline solution," *Physical Chemistry Chemical Physics*, vol. 10, no. 25, pp. 3802–3811, 2008.
- [26] C. Z. Li, A. Bogozi, W. Huang, and N. J. Tao, "Fabrication of stable metallic nanowires with quantized conductance," *Nanotechnology*, vol. 10, no. 2, pp. 221–223, 1999.
- [27] H. X. He, S. Boussaad, B. Q. Xu, C. Z. Li, and N. J. Tao, "Electrochemical fabrication of atomically thin metallic wires and electrodes separated with molecular-scale gaps," *Journal of Electroanalytical Chemistry*, vol. 522, no. 2, pp. 167–172, 2002.
- [28] A. Gross, "Adsorption at nanostructured surfaces," in *Handbook of Theoretical and Computational Nanotechnology*, chapter 89, American Scientific Publishers, 2006.
- [29] E. Santos, P. Quaino, and W. Schmickler, "On the electrocatalysis of nanostructures: monolayers of a foreign atom (Pd) on different substrates M(1 1 1)," *Electrochimica Acta*, vol. 55, no. 14, pp. 4346–4352, 2010.
- [30] B. Hammer and J. K. Nørskov, "Theoretical surface science and catalysis—calculations and concepts," *Advances in Catalysis*, vol. 45, pp. 71–129, 2000.
- [31] E. Santos, P. Quaino, G. Soldano, and W. Schmickler, "Electrochemical reactivity and fractional conductance of nanowires," *Electrochemistry Communications*, vol. 11, no. 9, pp. 1764–1767, 2009.
- [32] G. J. Soldano, P. Quaino, E. Santos, and W. Schmickler, "Stability of gold and platinum nanowires on graphite edges," *ChemPhysChem*, vol. 11, no. 11, pp. 2361–2366, 2010.
- [33] P. Quaino, E. Santos, H. Wolfschmidt, M. Montero, and U. Stimming, "Theory meets experiment: electrocatalysis of hydrogen oxidation/evolution at Pd-Au Nanostructures," *Catalysis Today*. In Press.



**Hindawi**

Submit your manuscripts at  
<http://www.hindawi.com>

